

# Rings and spirals in barred galaxies. III. Further comparisons and links to observations.

E. Athanassoula<sup>1</sup>, M. Romero-Gómez<sup>1,2</sup>, A. Bosma<sup>1</sup>, J.J. Masdemont<sup>3</sup>

<sup>1</sup>Laboratoire d'Astrophysique de Marseille (LAM), UMR6110, CNRS/Université de Provence,

Technopôle de Marseille Etoile, 38 rue Frédéric Joliot Curie, 13388 Marseille Cédex 20, France

<sup>2</sup>Institut de Ciències del Cosmos, IEEC-UB, Universitat de Barcelona, Martí Franquès 1, 08028 Barcelona, Spain

<sup>3</sup>IEEC & Dep. Mat. Aplicada I, Universitat Politècnica de Catalunya, Diagonal 647, 08028 Barcelona, Spain

Received

## ABSTRACT

In a series of papers, we propose a theory to explain the formation and properties of rings and spirals in barred galaxies. The building blocks of these structures are orbits guided by the manifolds emanating from the unstable Lagrangian points located near the ends of the bar. In this paper, the last of the series, we present more comparisons of our theoretical results to observations and also give new predictions for further comparisons. Our theory provides the right building blocks for the rectangular-like bar outline and for ansae. We consider how our results can be used to give estimates for the pattern speed values, as well as their effect on abundance gradients in barred galaxies. We present the kinematics along the manifold loci, to allow comparisons with the observed kinematics along the ring and spiral loci. We consider gaseous arms and their relations to stellar ones. We discuss several theoretical aspects and stress that the orbits that constitute the building blocks of the spirals and rings are chaotic. They are, nevertheless, spatially well confined by the manifolds and are thus able to outline the relevant structures. Such chaos can be termed ‘confined chaos’ and can play a very important role in understanding the formation and evolution of galaxy structures and in galactic dynamics in general. This work, in agreement with several others, argues convincingly that galactic dynamic studies should not be limited to the study of regular motions and orbits.

**Key words:** galaxies – structure – ringed galaxies – barred galaxies

## 1 INTRODUCTION

In previous papers (Romero-Gómez *et al.* 2006, hereafter Paper I; Romero-Gómez *et al.* 2007, hereafter Paper II; Athanassoula, Romero-Gómez & Masdemont 2009a, hereafter paper III; Romero-Gómez *et al.* 2009) we proposed a theory to explain the formation and structure of spirals and inner and outer rings in barred galaxy potentials. We propose that the building blocks of these structures are chaotic orbits that are guided by manifolds associated with the Lagrangian points  $L_1$  and  $L_2$  which are located along the direction of the bar major axis. These manifolds can be thought of as tubes that confine the orbits, so that the latter can form thin structures in configuration space.

A theory, however, can be dynamically correct but still irrelevant to a particular application. We therefore have to check whether our theory is applicable to spirals and rings observed in barred disc galaxies. It is thus necessary to compare our theoretical results and predictions to observations. We started this in Paper IV (Athanassoula *et al.* 2009b, hereafter Paper IV) where we made a number of comparisons of model spirals and rings, the latter both inner and outer, to observations and found good agreement. We found that our theory can reproduce all necessary morphologies of

both inner and outer rings, and produces no unrealistic morphologies. Model inner rings were found to be elongated along the bar and outer ones either along it ( $R_2$ , or  $R'_2$ ), or perpendicular to it ( $R_1$ , or  $R'_1$ ), or both ( $R_1 R_2$ ).

Model spirals in barred galaxy potentials were found to be predominantly two-armed and trailing, although arms of higher multiplicity are possible for specific potentials. They were found to have the right shape and could reproduce the fall-back of an arm towards the bar region or towards the other arm, which is observed in many spirals. A quantitative comparison to the arm shapes of NGC 1365 proved successful. We predict that the relative strength of the non-axisymmetric forcing in the region around and somewhat beyond corotation influences the winding of the arms, in the sense that in strongly barred galaxies the spirals will be more open than in less strongly barred ones. Thus, a series of models with increasing bar strength will have a continuous sequence of morphologies from  $R_1$  to  $R'_1$ , then to tightly wound spirals, to end with open spirals. We also compared the shape of the inner and outer rings, as well as the ratio of outer-to-inner ring major axes of our models to observations and discussed which type of potentials give best agreement. We also showed that there are correlations, or trends, between all

the ratios of ring sizes discussed above and the bar strength. These correlations are very tight if only one type of model potential is used but thicken, sometimes very considerably, if other models, with different properties and analytical expressions, are included.

The present paper is the fifth and last of this series. A reminder of the main theoretical results and prerequisites is given in Sect. 2. This is very brief, since these concepts have been described extensively in Papers I, II and III. Here we will mainly present further comparisons with observations and predictions. These include e.g. the bar shape (Sect. 3.1), ansae (Sect. 3.2), radial drift and abundance gradients (Sect. 3.3). Kinematics and behaviour of the line-of-sight velocities are discussed in Sect. 4 and pattern speed prediction is the subject of Sect. 5. In Sect. 6 we discuss specific topics, such as time evolution, self-consistency and spiral structure formation, and we also compare with other spiral structure theories and give outlines for further work. These discussions rely on material from all five papers in this series. Finally, we summarise and conclude in Sect. 7.

## 2 THEORETICAL REMINDERS

Our theory relies to a large extent on the dynamics of the Lagrangian points  $L_1$  and  $L_2$  of a two-dimensional barred galaxy system. These points are located along the direction of the bar major axis and are, in the standard case, saddle point unstable (Binney & Tremaine 2008). Their distance from the centre is denoted here by  $r_L$  and it is referred to as corotation, or Lagrangian radius. Each of them is surrounded by a family of periodic orbits, called Lyapunov orbits (Lyapunov 1949). Since these are unstable they can not trap around them quasi-periodic orbits of the same energy<sup>1</sup>, so that any orbit in their immediate vicinity (in phase space) will have to escape the neighbourhood of the corresponding Lagrangian point. Not all departure directions are, however, possible. The direction in which the orbit escapes is set by what we call the invariant manifolds. These can be thought of as tubes that guide the motion of particles of the same energy as the manifolds (Gómez et al. 2004; Koon et al. 2000). Each manifold has four branches emanating from the corresponding Lyapunov orbit, two of them inside corotation (inner branches) and two of them outside (outer branches). Along two of these branches (one inner and one outer) the mean motion is towards the region of the Lagrangian point (stable manifolds), while along the other two it is away from it (unstable manifolds). We need to stress that the terms ‘stable’ and ‘unstable’ do not mean that the orbits that follow them are stable and unstable, respectively. In fact all the orbits that follow the manifolds are chaotic, but they are in a loose way ‘confined’ by the manifolds, so that they stay together, at least for a few bar rotations, in what could be called a bundle. These manifolds do not exist for all values of the energy, but only for energies for which the corresponding Lyapunov periodic orbit is unstable. This means energies within a range starting from the energy of the  $L_1$  or  $L_2$  ( $E_{J,L_1}$ ) and extending over a region whose extent depends on the model (Skokos, Patsis & Athanassoula 2002). In this series of papers we propose that these manifolds and orbits are the building blocks of the spirals and rings in barred galaxies.

As shown in Papers II and III, the properties of the manifolds depend strongly on the relative strength of the non-axisymmetric

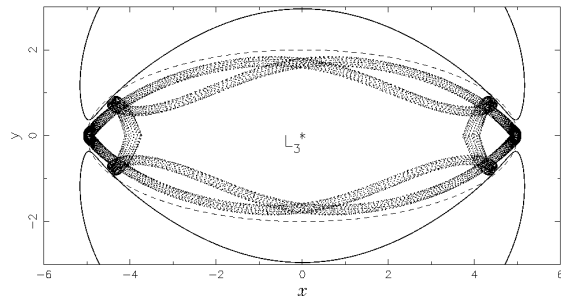


**Figure 1.** Shapes outlined by the inner manifolds after half a revolution around the galactic centre for a model with strongly unstable  $L_1$  and  $L_2$  Lagrangian points. We see that these provide building blocks for a rectangular-like outline of the bar. The dashed line traces the outline of the Ferrers potential and the solid lines the curves of zero velocity for the same energy as the manifolds. The centre of the galaxy, where the  $L_3$  Lagrangian point is located, is marked with a star.

forcing at and somewhat beyond corotation. We measure this with the help of the quantity  $Q_{t,L_1}$ , which is the value of  $Q_t$

$$Q_t(r) = (\partial\Phi(r, \theta)/\partial\theta)_{max}/(r\partial\Phi_0/\partial r), \quad (1)$$

at  $r_L$ , the radius of the Lagrangian point  $L_1$  or  $L_2$ , i.e.  $Q_{t,L_1} = Q_t(r = r_L)$ . This is not the same as the strength of the bar, which is often measured by  $Q_b$ , i.e. the maximum of  $Q_t$  over all radii shorter than the bar extent. The radius at which this maximum occurs can be small compared to  $r_L$ . So  $Q_b$  is not necessarily a good proxy for  $Q_{t,L_1}$  and vice versa. Nevertheless, for the sake of brevity, we will often replace in our discussions “non-axisymmetric forcings which are relatively strong at and beyond corotation” simply by “strong bars”, or “strong non-axisymmetric forcings”.

The models used here are described extensively in an appendix of Paper III. Model A is taken from Athanassoula (1992a) and has a Ferrers bar (Ferrers 1877) of semi-major axis  $a$ , axial ratio  $a/b$ , quadrupole moment  $Q_m$  and rotating with a pattern speed  $\Omega_p$ . The central concentration of this model is characterised by its central density  $\rho_c$ . The fiducial model of this series of papers has the parameter values  $Q_m = 4.5 \times 10^4$ ,  $a/b = 2.5$ ,  $r_L = 6$ ,  $a = 5$ ,  $\rho_c = 2.4 \times 10^4$  and  $n = 1$ . The units are  $10^6 M_\odot$ , 1 kpc and 1 km/sec, for the mass, length and velocity, respectively. Model D has a Dehnen-like bar potential (Dehnen 2000) characterised by a strength parameter ( $\epsilon$ ) and a scale length ( $\alpha$ ). The BW model has a bar with a Barbanis & Woltjer type potential (Barbanis & Woltjer 1967) characterised by a strength parameter ( $\hat{\epsilon}$ ) and a scale length ( $r_1$ ). As in the previous papers, we use the two latter models to represent forcings not only from bars, but also from spirals, oval discs and triaxial haloes.

Unless otherwise stated, we use in this series of papers a frame of reference corotating with the bar, because calculations are more straightforward in this frame. We measure angles in the standard mathematical sense, i.e. starting from the positive  $x$  axis and increasing anticlockwise.

## 3 FURTHER COMPARISONS WITH OBSERVATIONS

### 3.1 Bar shape

Athanassoula et al. (1990) showed that the isodensities of the outer bar region of early type, strongly barred galaxies have predominantly a rectangular-like shape. This was later confirmed for larger

<sup>1</sup> We will all through this paper loosely call ‘energy’ the numerical value of the Hamiltonian in a frame of reference co-rotating with the bar, i.e. a frame in which the bar is at rest, and denote it by  $E_J$ .

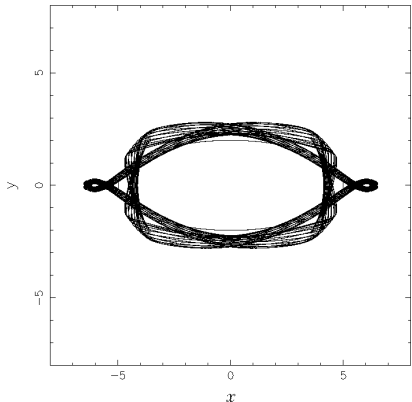


**Figure 2.** The inner manifolds for a model with stable  $L_1$  and  $L_2$  Lagrangian points (see Paper III). It is clear that these provide building blocks for a rectangular-like outline of the bar, as well as for ansae.

samples by Gadotti (2008, 2010) and for bars in  $N$ -body simulations by Athanassoula & Misiriotis (2002). The origin of this shape has been widely debated. A first obvious possibility, already discussed by Athanassoula *et al.* (1990), is that the rectangularity is due to orbits trapped around the periodic orbits in the vicinity of inner ultraharmonic (4:1) resonance. This, however, could only be true if the corresponding periodic orbits are stable, which is not generally true (Contopoulos 1988; Athanassoula 1991, 1996; Patsis *et al.* 1997). Athanassoula (1991, 1996) proposed alternative solutions, like trapped regular orbits wobbling around  $x_1$  periodic orbits, superposition of orbits trapped around two families of 3:1 periodic orbits symmetric with respect to the bar minor or major axis, or chaotic orbits confined by cantori, i.e. orbits staying for long times around unstable rectangular-like 4:1 orbits. All these alternatives were examined in detail in the potential of NGC 4314 (Patsis *et al.* 1997).

Our work here argues that the role of chaotic orbits in explaining this rectangular-like shape is crucial. Indeed, in Paper III we discussed the inner branches of the manifolds and showed that their properties depend on the bar strength. For weak bars, if we trace the inner manifolds over more than half a revolution around the galactic centre, then the manifolds retrace the same loci, forming an inner ring. On the other hand, for strong bars, the inner manifolds cover a new path after the first revolution around the galactic centre and retrace the same loci only after a couple or a few revolutions. An example of the latter is shown in Fig. 1. The bar here is strong ( $Q_m = 7$  and  $r_L = 5$ , the values of the remaining parameters being the same as for the fiducial model) and it is clear that the orbits corresponding to such manifolds can provide building blocks for the rectangular outline of the bar. Fig. 2 shows another example, this time from a case with stable  $L_1$  and  $L_2$  Lagrangian points (Paper III). In this case also, the inner manifold branches can provide useful building blocks for the rectangular bar outline.

In both these examples, and in all the other models we tried, considerable parts of the inner manifold branches can outline the outer part of the bar so that this rectangularity of the isodensities should be expected to occur in the outer parts of the bar. This is indeed what is seen both from the observations (Athanassoula *et al.* 1990) and the simulations (Athanassoula & Misiriotis 2002). As discussed in Paper III, such building blocks for rectangular-like bar outlines should be seen mainly in strong bars and this again is in good agreement with both observations (Athanassoula *et al.* 1990;

Gadotti 2008, 2010) and simulations (Athanassoula & Misiriotis 2002).

To summarise, the inner manifold branches can produce the right building blocks for the rectangular-like outline of the outer parts of strong bars.

### 3.2 Ansae

Ansae are concentrations of matter located at both ends of the bar (Sandage 1961; Athanassoula 1984; Martinez-Valpuesta, Knapen & Buta 2007). Manifolds can, in some cases, contribute the right building blocks for this structure as well. In general, the  $L_1$  and  $L_2$  are unstable. In Paper III, however, we showed that if there are mass concentrations centred on these unstable Lagrangian points, then the  $L_1$  and  $L_2$  can become stable, provided these masses are sufficiently massive and concentrated. In this case, four other unstable points will appear on the direction of the bar major axis, one on each side of the  $L_1$  and of the  $L_2$ . There are thus seven rather than three Lagrangian points on the  $x$  axis (i.e. the direction of the bar major axis). The central one ( $L_3$ ), two at smaller radii than the  $L_1$  and  $L_2$  (which we call  $L_1^i$  and  $L_2^i$ , where  $i$  stands for inner) and two at larger radii (which we call  $L_1^o$  and  $L_2^o$ , where  $o$  stands for outer). In such configurations, part of the manifold, emanating from  $L_1^i$  or  $L_1^o$  (respectively  $L_2^i$  or  $L_2^o$ ), encircles the  $L_1$  (or  $L_2$ ). This part of the manifolds, together with regular orbits trapped around the now stable Lyapunov orbits can be the building blocks for ansae (Fig. 2).

### 3.3 Motions within the galaxy and abundance gradients

As already discussed in Papers I to III, the  $L_1$  and  $L_2$  Lagrangian points can be considered as gateways through which material from within corotation can move to larger radii outside corotation and vice versa. In general, this will induce considerable radial motion within the galaxy and will therefore partly smooth out abundance gradients. We will discuss here in more detail two specific cases, an  $rR_1$  morphology and a spiral morphology. As usual, we place ourselves in a frame of reference rotating with the bar. In this frame of reference the sense of rotation in the outer ring, be it  $R_1$  or  $R_2$ , is clockwise, i.e. retrograde. On the other hand, it is anticlockwise, i.e. direct in this frame, for the inner manifold branches, i.e. for the inner ring, or the outer parts of the bar.

A star trapped by manifolds resulting in an  $rR_1$  morphology can follow four different paths. In the first one, illustrated in the left panel of Fig. 3, the star will be guided solely by the inner manifold branches. It will thus trace the inner ring, or the outer part of the bar, without moving to regions further out. Such motions have been found in many cases, both for models and observations, as e.g. in the hydrodynamic models of IC 4214 by Salo *et al.* (1999). They will only smooth out abundance gradients within the outer parts of the bar.

In the second alternative, illustrated in the central panel of Fig. 3, the star will be guided solely by the outer manifold branches. If most stars followed such paths, there would be some smoothing of the abundance gradients because the paths are far from circular, but this smoothing would be considerably less than what will occur for the paths described below, since it concerns only an annulus outside corotation.

The third path, illustrated in the right panel of Fig. 3, is more complex. A mass element near  $L_1$  will move on the inner branch

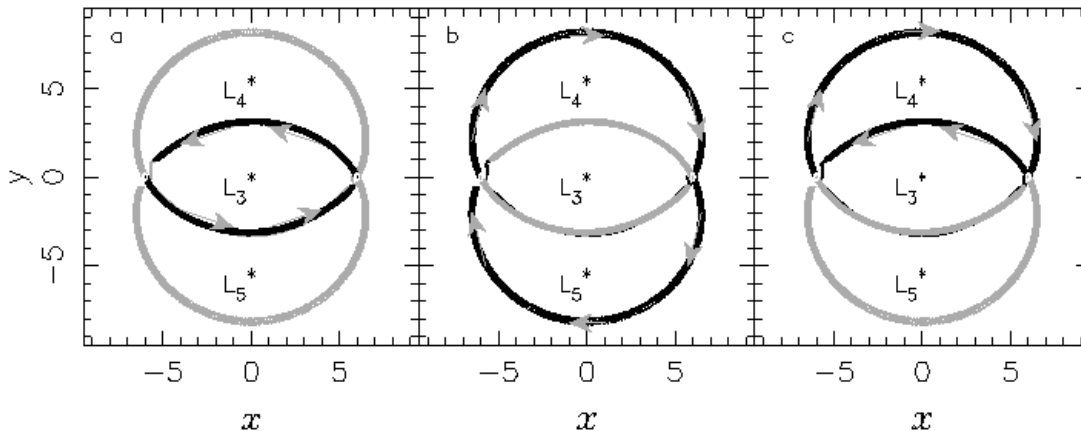


**Figure 3.** Three possible circulation patterns for particles on orbits guided by the manifolds in an example with an  $rR_1$  morphology. Any given such particle can stay on the inner branches of the manifold, i.e. can trace the inner ring (left panel), or it can stay on the outer branches of the manifold, i.e. can trace the outer ring (middle panel). Alternatively, it can trace a path that includes one inner and one outer branch. Two such paths are possible. One is shown in the right panel. The other, i.e. the fourth alternative, is not plotted here since it is similar to the third one, except that it is symmetric with respect to the bar major axis. After a particle has completed a full circulation path, it can either repeat the same path, or take any of the other three ones. The manifolds coming into play in each case are plotted in black in the corresponding panel, and the remaining ones in light grey. In white, we plot the Lyapunov periodic orbits of the corresponding energy level. The arrows show the direction of the motion. This particular model has  $Q_m = 8$  and  $r_L = 6$ , the remaining parameters being the same as for the fiducial model. Similar results, however, are found for all  $rR_1$  morphologies.

away from  $L_1$  and towards  $L_2$ . When it reaches the vicinity of  $L_2$  it will leave it, guided by the unstable outer manifold branch. It will thus move outwards until it reaches a maximum radius and then continue inwards towards  $L_1$  on the stable outer manifold branch to reach again the vicinity of  $L_1$  from which it started. The sense of the motion is clockwise with respect to the Lagrangian point  $L_4$ , which is enclosed within it. The fourth alternative is similar to the third one. Its loci are the mirror image of those of the third one with respect to the bar major axis and the sense of rotation is clockwise with respect to  $L_5$ . For the last two paths, the radial mixing of material concerns a region which is radially much more extended than for the first two and could thus smooth out considerably any radial abundance gradients. Even so, this will not concern material at radii smaller than the minor axis of the inner ring or larger than the major axis of the outer ring. Once a star has completed one path it can continue on the same path following again the same circulation pattern, or it can take any of the other three paths. Thus a star can first go around the inner ring, then around the outer ring and then follow a mixed trajectory, or any other sequence of the four possible circulation patterns.

If instead of an  $rR_1$  we have a spiral morphology, then the circulation pattern is much simpler and the amount of radial mixing yet more important. Material moves along one of the inner stable manifold branches towards one of the unstable Lagrangian points  $L_1$  or  $L_2$ . Since for spirals the non-axisymmetric forcing is strong, the inner manifolds traverse regions of the bar located at a relatively small distances from the centre and thus can guide bar material from these regions outwards (see Fig. 4). Such material will then continue outwards along the spiral, so that, starting from well within the bar, it will reach radii very far from the centre. In such cases, the radial mixing concerns a very large radial extent and this outgoing material can, furthermore, extend the disc outwards. This motion should also reduce considerably any abundance gradients in these regions. It is, however, not possible to make more precise predictions about the abundance gradients, unless a full model is built, including the abundance gradients before the bar was introduced.

Martin & Roy (1994) studied abundance gradients in disc

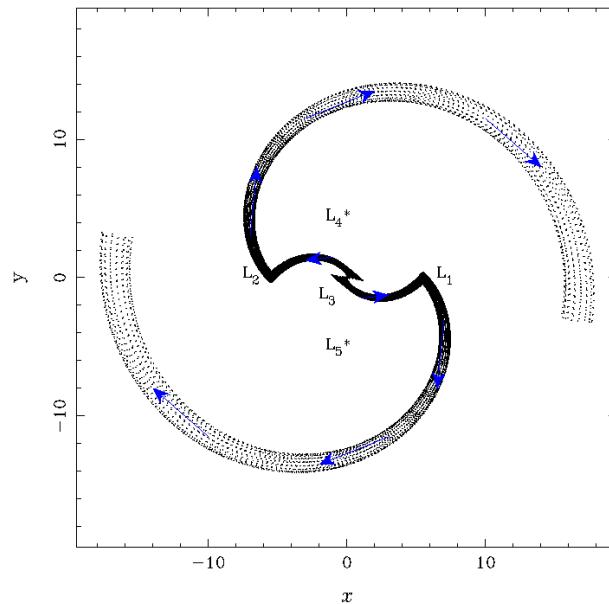


**Figure 4.** Circulation patterns for particles in a model with spiral morphology. Such patterns induce very strong radial mixing, since material from very near the galactic centre can reach regions far out in the disc.

galaxies and found that these are shallower in barred than in non-barred ones. They furthermore found that the strength of the bar plays a determining role: the flatter gradients are found in galaxies with stronger bars. These results are in very good agreement with our theory. Indeed, circulation of material driven by the manifolds will render abundance gradients shallower. For bar strengths below a given threshold the morphology is  $rR_1$  (Paper III) and, as we saw above, in such cases the region in which the radial mixing occurs is set by the elongation of the rings. Furthermore, both observations and theory (Paper IV), show that rings are more elongated when the bars are stronger. Therefore, in more strongly barred

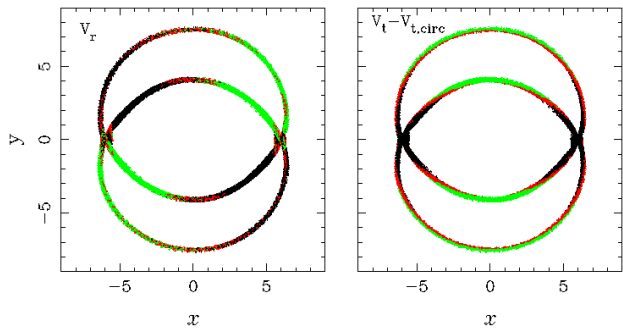


**Figure 5.** Radial (left panel) and tangential velocities (after subtraction of the circular velocity – right panel) along the inner and outer rings of an  $rR_1$  morphology case. The velocities are calculated in an inertial frame of reference. Positive values are given in black and negative in green. Values around zero, more precisely in the  $(-2.5, 2.5)$  bracket, are given in red.

galaxies the radial mixing will occur over regions which are more radially extended and thus lead to flatter abundance gradients. For yet stronger bars the manifolds will drive a spiral morphology, in which, as discussed above, the radial mixing will concern yet larger regions. Thus our theoretical results are in good agreement with observations on this point.

#### 4 KINEMATICS

Kinematics can provide very strong constraints in comparisons between models and observations. For this reason, we discuss in this section the velocities along the orbits guided by the manifolds in two specific morphologies, the  $rR_1$  rings and the spirals, which are the most frequently observed cases (Buta 1995) and are also the most interesting dynamically. Since our aim here is to provide measurements that can be compared with observations, we will calculate the velocities in the inertial frame of reference.

Fig. 5 gives information on the motion along the manifolds in the case of an  $rR_1$  morphology<sup>2</sup>. The model here, as well as in Figs. 6 and 7, is the fiducial A model. It has  $Q_{t,L_1} = 0.038$  and its inner and outer rings have axial ratios of 0.81 and 0.90, respectively. However, results from other models with a similar morphology are qualitatively the same. As expected from the results presented so far and as can be seen in the left panel of Fig. 5, along the outer ring the motions is outwards in the upper left quadrant of the ring and inwards in the upper right part. Zero radial velocity is reached roughly at the direction of the major axis of the outer ring. This is in agreement with the fact that the motion is outwards (i.e. away from the Lagrangian point from which the manifold emanates) along the unstable manifold branches and inwards along the stable ones (Papers I, II and III).

In order to show best the perturbations of the tangential velocity, we subtract from it the circular velocity calculated at the radius at which the measurement is made. The result is given in the right panel of Fig. 5. This shows that, in general, the tangential motion in the outer part of the ring is slower than in the inner part.

Fig. 6 shows, for each ring separately, the radial and tangential components of the velocity, calculated as above along the ring,

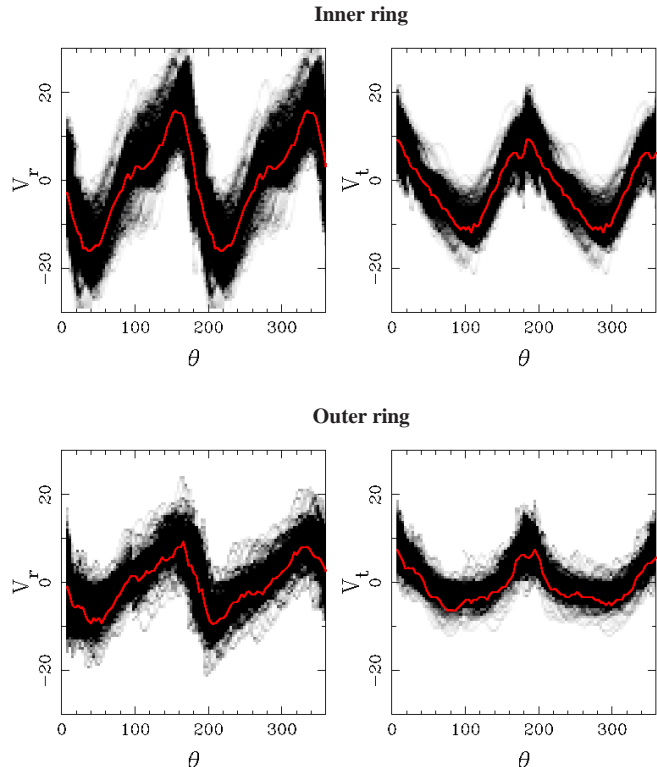


**Figure 6.** Radial (left panels) and tangential velocities (after subtraction of the circular velocity – right panels) along the inner (upper panels) and outer (lower panels) rings. The model is the same as in Fig. 5. The median values as a function of the angle are given by the red curve.

but now plotted as a function of the azimuthal angle. In both cases, both velocity components show an oscillation of an amplitude less than or of the order of 20 km/sec. Also, in both cases the oscillation has two maxima and two minima, but is not sinusoidal. The radial velocity curve is asymmetric, in the sense that the angular extent over which the radial velocity increases with increasing angle is more extended than that over which it is decreasing. Some of these results could have been directly obtained from the manifold analyses done so far (see e.g. Fig. 3). Material leaving the  $L_1$  or the  $L_2$  Lagrangian point will move away from it on the unstable manifold branches. Since the major axis of the outer ring is oriented perpendicular to the bar, this means that the radial velocity will be positive until roughly  $90^\circ$  for the  $L_2$ , or  $-90^\circ$  for the  $L_1$ . After that, the sense of the radial motion is reversed and the particle will head for the Lagrangian point opposite to the one it started from. This explains the changes of sign in the lower left panel of Fig. 6. For the inner ring, both the sense of circulation (in the rotating frame of reference) and the directions of the major and minor axes are reversed, so that the variations of the sign of the velocity as a function of  $\theta$  stay globally the same. Fig. 6 also shows that the amplitude of the oscillations is larger for the inner than for the outer ring, which should be linked to the fact that the bar forcing is stronger at the inner ring radii than at the outer ring and the inner ring is more elongated than the outer one (for observed rings see Buta 1995, and for theoretical ones see Paper IV, Sect. 5).

The tangential velocities, calculated in the inertial frame of reference and after subtraction of the circular velocity, are given in the right panels of Fig. 6. Again, the maxima and minima occur at roughly the same angles for the inner and the outer rings and the

<sup>2</sup> Note that this is different from what is given in Mel'nik & Rautiainen (2005), where the velocities are measured in a circular annulus, only part of which corresponds with the ring. Their results, therefore, are not directly comparable to ours.

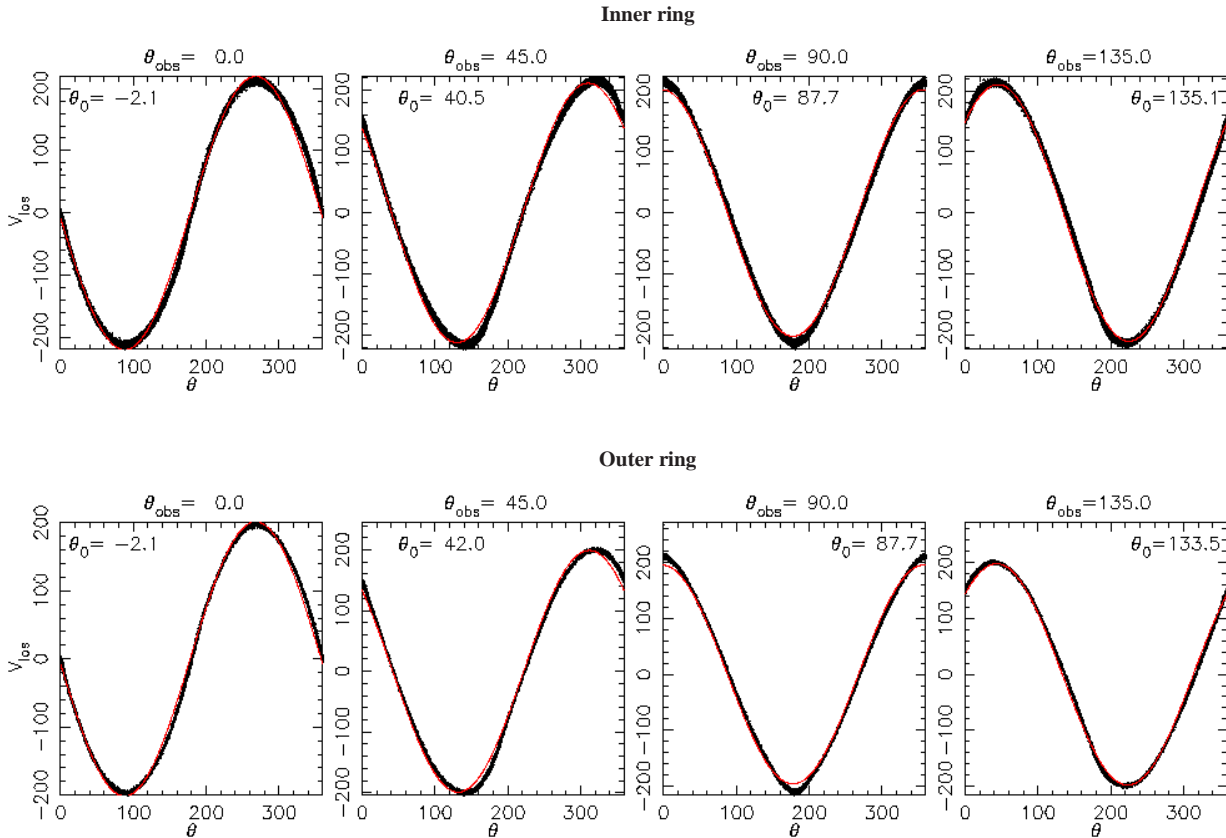


**Figure 7.** Line-of-sight velocity for points along the inner (upper row of panels) and outer (lower row of panels) ring in the case of an  $rR_1$  morphology. Each panel corresponds to a given viewing angle, whose value is given at the top of the panel. The models and orbits are as in Figs. 5 and 6. The red lines are the best fitting sinusoidal curves. All angles are in degrees.

amplitude of the oscillation is much larger for the inner than for the outer ring.

To compare with observations we need to calculate the component of the velocity along the line of sight,  $v_{los}$ . The results are given in Fig. 7, separately for the inner and the outer rings and for four viewing angles. The line-of-sight velocities look roughly sinusoidal, so, as is customary for observations, we fitted sine curves of the form  $A \sin(\theta - \theta_0)$  to them. The values of the amplitude  $A$  vary between 202 (for  $\theta_{obs} = 90^\circ$ ) and 219 (for  $\theta_{obs} = 0^\circ$  and  $180^\circ$ ) and the corresponding  $\theta_0$  values indicate the position at which the line-of-sight velocity is zero. The latter are very near the viewing angle of the observer and always lagging slightly behind it. The minimum deviation is less than a degree (for  $\theta_{obs} = 135$ ) and the maximum deviation around  $4^\circ$  (for  $\theta_{obs} = 45$ ). These values are in good agreement with the differences between the inner ring photometric and kinematic major axis position angles observed e.g. for NGC 6300 (Buta 1987) and NGC 1433 (Buta 1986). Similar results are found for the outer  $R_1$  ring (two bottom panels), but the amplitude varies little with  $\theta_{obs}$ .

Let us now look at the kinematics of a case with a somewhat stronger relative non-axisymmetric forcing, which, in agreement with what was found in Paper III, has also an  $rR_1$  morphology, but more elongated rings (minor-to-major axes ratios of 0.57 and 0.78 for the inner and outer rings, respectively). The model has the same parameters as the one we analysed above, but a  $Q_m = 9 \times 10^4$ . The radial and tangential velocities along the ring loci are given in Fig. 8. The main difference with the previous case is that the amplitude of the oscillations is much larger, so that the absolute

value of the radial velocity can go even higher than 50 km/sec at certain angles, while that of the peculiar tangential velocity can go as high as, or even exceed 25 or 30 km/sec.

Let us now consider a case with a much stronger relative non-axisymmetric forcing, which, in agreement with what was found in Paper III, has a spiral morphology. We will use a D model with parameters  $\epsilon = 0.3$  and  $r_L = 5$ , and we plot the radial and tangential velocities in Figs. 9 and 10 (left and right panels, respectively). Material on orbits emanating from the vicinity of  $L_1$  or  $L_2$  moves outwards with increasing radial velocity for the first roughly  $80^\circ$ , then the radial velocity reaches a maximum and starts decreasing. The material still moves outwards, however, up to a winding of roughly  $260^\circ$  at which point the radial velocity changes sign and the motion changes to inwards. Similar information for the tangential component of the velocity is given in the right panels of these figures. Material will move from  $L_1$  or  $L_2$  with a tangential velocity which is above the circular velocity until it has described roughly  $80^\circ$  and then will continue with a smaller tangential velocity. After about one rotation, however, the tangential velocity will stay at a roughly constant value.

From the cases described above, and from a number of others which we have run but do not show here, we see that there is a continuity between the kinematics of material along  $R_1$  rings and kinematics along spirals, with, nevertheless, clear quantitative differences. For example, for stronger relative non-axisymmetric forcings the radial velocity changes sign much further along the arm i.e. further away from the Lagrangian point from which the arm emanates. Let us call the angle at which this change occurs  $\theta_{cs}$ . It is

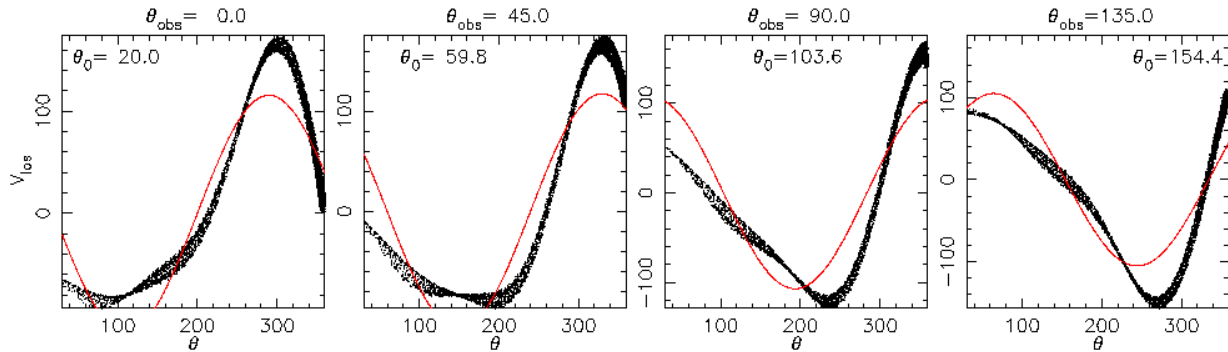


**Figure 11.** Line-of-sight velocity for points along one of the spiral arms for the model shown in Figs. 9 and 10. Each panel corresponds to a given viewing angle, whose value is given in the top of the panel. All angles are in degrees. The red lines are the best fitting sinusoidal curves, which in all these cases are poor fits.

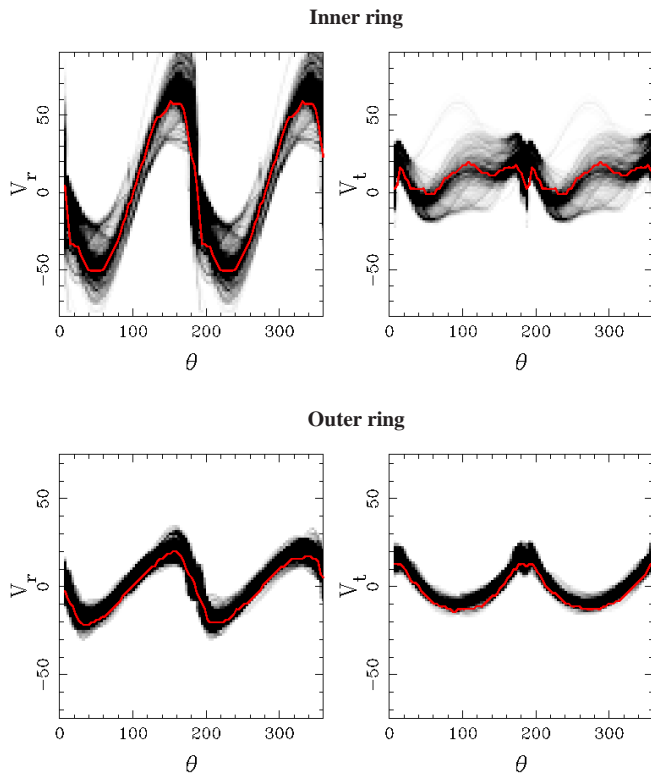


**Figure 8.** As Fig. 6, for a model with a stronger bar ( $Q_m = 9 \times 10^4$ ), but still with an  $rR_1$  morphology. The red curve gives the median value as a function of the angle.

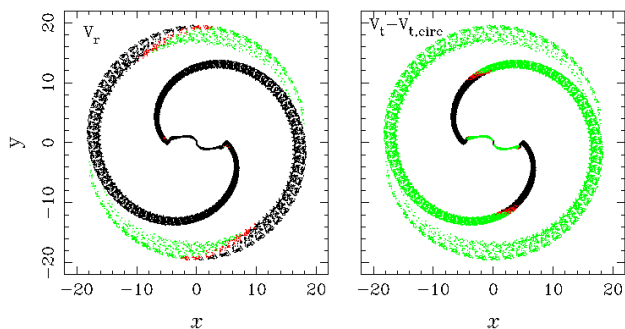


**Figure 9.** As in Fig. 5 but the velocities are now calculated along the spiral arms of a D model with  $\epsilon = 0.3$  and  $r_L = 5$ .

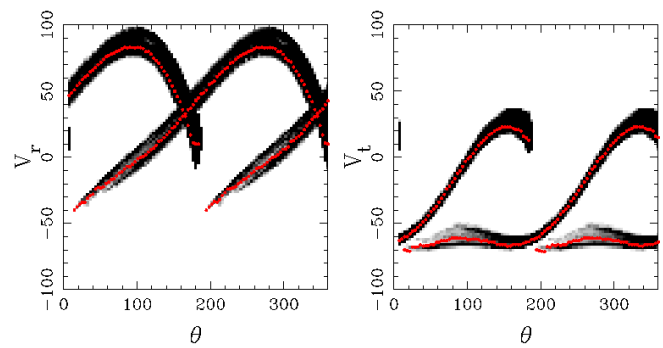


**Figure 10.** Radial (left panel) and tangential velocities (after subtraction of the circular velocity – right panel) along the spiral of a D model with  $\epsilon = 0.3$  and  $r_L = 5$ . The red curve gives the median values.

measured from the Lagrangian point from which the manifold emanates in the sense in which the particles are moving. The A model described in Figs. 5 and 6 has  $Q_{t,L_1} = 0.038$  and  $\theta_{cs} = 80^\circ$ , while the A model described in Fig. 8 has  $Q_{t,L_1} = 0.072$  and  $\theta_{cs} = 90^\circ$ . A D model with  $\epsilon = 0.25$  and  $r_L = 5$ , has  $Q_{t,L_1} = 0.515$  and  $\theta_{cs} = 230^\circ$ , while the D model with  $\epsilon = 0.3$  and  $r_L = 5$  (Figs. 9 and 10) has  $Q_{t,L_1} = 0.618$  and  $\theta_{cs} = 255^\circ$ . From these and other models we see that there is definitely a trend, but it is beyond the scope of this paper to see whether this is a tight correlation and whether this is model dependent. Similar trends can be found also for the tangential velocity. To what extent this result can be modified by self-consistent calculations is still unclear.

Another difference can be seen by comparing Figs. 7 and 11. The former shows that for both inner and outer rings and for all values of the viewing angle the line-of-sight velocity can be well fitted by a sinusoidal curve. Fig. 11 gives the line-of-sight velocity for the spiral case. The velocities are now measured along the spiral arm. One sees clearly that in this case a sinusoidal is a bad fit to the data and should not be used to find the galaxy major axis.

## 5 PATTERN SPEED PREDICTION

The pattern speed, i.e. the angular velocity of the bar, conditions strongly the dynamics within a barred galaxy. Unfortunately it can not be directly observed and it is thus necessary to resort to indirect, and often rather convoluted methods, to obtain its value. Orbital structure studies of barred galaxies have shown that a bar can not extend beyond its corotation (Contopoulos 1980). A sim-

ilar result was reached from the calculation of the self-consistent response to a bar forcing (Athanassoula 1980). These two results are very useful, since they set a lower limit to the corotation radius, which can thus not be smaller than the bar length, but give no information on an upper limit. A two-sided constraint, i.e. one limiting the Lagrangian radius from both smaller and larger radii, has been found from the comparison of shock loci in hydrodynamic simulations and dust lane loci observed in barred galaxies. The possible range for the Lagrangian radius is thus found to be  $r_L = (1.2 \pm 0.2)a$ , where  $a$  is the bar semimajor axis (Athanassoula 1992b). This has proved to be the tightest constraint to date and compares well with observational results (Elmegreen 1996), the most extensive of which are from the application of the Tremaine-Weinberg method (Tremaine & Weinberg 1984) to bright early type galaxies (Aguerri, Debattista & Corsini 2003; Gerssen, Kuijken & Merrifield 2003; Corsini & Debattista 2009 and references therein). Yet the observational errors for all methods are rather large and more precise determinations would be desirable (Corsini & Debattista 2009). We will examine here whether, and in what cases, our work could provide some input on pattern speed values. Indeed, from all the above and from Papers I, II and III it is clear that the position of the Lagrangian points is intimately linked with the morphology and thus can perhaps be estimated from it.

If the galaxy has a bar and no spiral, then the potential is symmetric with respect to both the bar major and minor axes and the  $L_1$  and  $L_2$  are on the direction of the bar major axis. If its morphology is  $rR_1$  and the inner and outer rings join, then the  $L_1$  and  $L_2$  are located at the position where the two rings join. If they do not join, but have a considerable distance between them, then the  $L_1$  and  $L_2$  can be stable, as discussed in Section 5 of Paper III. In this case, the Lagrangian points are situated in between the extremity of the inner ring major axis and the dimple of the outer ring. Taking it half way between the two is a good approximation. If the galaxy morphology is  $R_1R_2$ , the  $L_1$  and  $L_2$  can be localised in the same way as for the  $rR_1$ .

In cases where the galaxy has an  $R_1$  outer ring with a clearly visible dimple but no inner ring, or the inner ring is not clearly delineated, the Lagrangian points should be in between the dimple and the tip of the bar major axis, but their exact location is difficult to pinpoint, unless a full model of the galaxy is made. The most difficult case is if the inner ring does not exist, or is very badly delineated, and at the same time the outer ring shows no clear dimples. In such a case the Lagrangian points should be on the direction of the bar major axis, between the end of the bar and the outer ring. Locating them half way between the two is the best guess, but has a large relative error. Even in such cases, however, this method can be useful since it gives some, albeit rough, estimate of the pattern speed very fast, simply from a galaxy image and without any need for kinematic observations.

In cases of barred galaxies with no rings and a relatively weak spiral structure emanating from the end of the bar, then the  $L_1$  (or  $L_2$ ) is located at the tip of the bar, where the arm joins the bar. In some cases this may be somewhat difficult to determine precisely in observations, since the distinction between the end of the bar and the beginning of the arm is not always easy to make. Nevertheless the error this entails is not very large. Cases where the spirals do not come directly out of the tip of the bar major axis are less clear cut.

$R_2$  morphologies with a spiral between the inner ring (or bar) and the outer ring, as ESO 325-28 (see third column of Fig. 2 in Paper IV), can be considered in the same way as simple spirals.

Cases with only an  $R_2$  ring do not present sufficient morphological characteristics to allow measurements of the  $L_1$  and  $L_2$  accurately. And of course nothing can be said from morphology alone about cases with no spirals and no rings.

An interesting peculiarity can happen in the case where the contribution of the spiral to the forcing is considerable. Contrary to the bar-only case, in bar-plus-spiral cases the iso-effective potential curves will not be symmetric with respect to the bar major and minor axes, since the spiral contribution lacks that symmetry. The Lagrangian points  $L_1$  and  $L_2$  would then not be located on the direction of the bar major axis, but at an angle to it. Stronger spirals will result in larger angles and trailing spirals will make clockwise displacements (leading spirals anticlockwise). This means that, if the spiral is sufficiently strong compared to the bar, corotation will not be exactly at the position where the bar joins the arm, but can be somewhat further down the arm. In such a case and at that location, the position of the dust lane will shift from the inside to the outside of the arm. Such a shift has indeed been observed in the SE arm of NGC 1365 (Ondrechen & van der Hulst 1989; Jörsäter & van Moorsel 1995), thus bringing corotation to  $1.4a$ , where  $a$  is the bar semimajor axis. This value is in good agreement with the value found from the hydrodynamical modelling of NGC 1365 (Lindblad, Lindblad & Athanassoula 1996; Zånmar Sánchez et al. 2008), and is within the bracket set by the gas flow simulations of Athanassoula (1992b), namely  $r_L = (1.2 \pm 0.2)a$ .

Once the Lagrangian points  $L_1$  and  $L_2$  have been clearly located, it is in principle straightforward to obtain the pattern speed. From the rotation curve one can obtain the curve  $\Omega = \Omega(r)$  and its numerical value at  $r = r_L$  is the pattern speed  $\Omega_p$ . In cases with strong bars, however, the position-velocity curves along and perpendicular to the bar major axis differ considerably (see e.g. Duval & Athanassoula (1983) for NGC 5383). Yet, and as can be seen e.g. from Fig. 16 in the afore mentioned paper, this difference is substantial mainly in the inner parts and considerably less so at the corotation region. Furthermore, if a sufficiently accurate velocity field is available, a yet more precise value of the pattern speed can be calculated from the rotation curve, since this is calculated from an azimuthal average of the velocities.

## 6 FURTHER DISCUSSION

### 6.1 Self-consistency and spiral structure formation

As discussed in Paper I (see particularly figure 6 there) the arm or outer ring forms gradually, from the Lagrangian point outwards. Any mass element needs some time to leave the vicinity of the  $L_1$  or  $L_2$  and to complete half a revolution around the galactic centre, and this time depends on the model. For strong bars this time is short, while for weak ones it is considerably longer. In Paper III we gave examples where this time varies roughly between 2 and 10 bar rotations. Furthermore, as shown in figure 6 of Paper I, the speed of formation depends strongly on the position along the arm. The part of the arm nearest to the Lagrangian point takes the longest to form and this time decreases with increasing distance from the arm origin.

In Paper III we showed that the bar strength plays a crucial role in determining the morphology and we gave a value which is a rough threshold between rings and spirals. Thus, bars less strong than this threshold will result in  $rR_1$  or  $rR'_1$  morphologies, and stronger ones in spirals. However, the time dependence discussed in



the previous paragraph argues that, in a fully self-consistent model in which time evolution is taken into account, the limits between the different morphologies will be shifted with respect to what we found in Paper III for simple rigid bar potentials where self-consistency is neglected.

To better understand this, let us consider a bar which has a strength somewhat below the limiting value necessary for the manifolds to have a spiral morphology, i.e. a bar strength given in Paper III as corresponding to an  $R_1$  or an  $R'_1$  outer ring. As we showed in Paper I (see particularly figure 6 there and corresponding discussion), the manifolds grow gradually from the  $L_1$  (or  $L_2$ ) outwards. At the initial stages of ring formation, only a segment of the ring has formed, so that the ring is not closed and looks like a short spiral arm. Its contribution, however, to the forcing is not taken into account in non-self-consistent simulations. So the evolution will give rise to the  $R_1$  or  $R'_1$  morphology which corresponds to the bar forcing.

On the other hand, in self-consistent simulations this segment will contribute an extra forcing which will foster a manifold with a spiral shape. The joint forcing of this ring segment and of the bar will drive manifolds which have a different shape than those that a bar only would drive, and are, in particular, more spiral-like. The resulting new segment, together with the bar, will give another manifold shape, etc, so that the final morphology can, in this case, be a trailing two-armed spiral. Thus, if the bar is sufficiently near the dividing line, it may have manifolds of a ring shape in non-self-consistent simulations and of spiral shape in self-consistent ones. As a result, the limiting bar strengths which divide the different types of manifold morphologies will be pushed downwards, to lower values of the bar strength. Fully self consistent simulations would be necessary in order to find out how much this shift will be.

## 6.2 Nature of the relevant orbits and differences between rings and spirals

As already discussed in the previous papers of this series, the orbits that constitute the building blocks of spirals and rings are chaotic. Yet they are spatially well confined by the manifolds, which can be thought of as tubes guiding the orbits. They can thus form features as narrow and as well defined as the spiral arms and rings observed in barred galaxies. For this reason, we propose to name this type of chaos ‘confined chaos’.

Intuitively, using chaotic orbits may seem a rather poor way of building narrow structures, since, given a sufficiently long time, chaotic orbits tend to cover all the phase space that is available to them (e.g. Contopoulos 2002). Yet the time required for this may be quite long, sometimes much longer than the time scale of the problem at hand, or even the Hubble time. Moreover, the phase space available to chaotic orbits is limited by the regions of phase space occupied by regular orbits and thus in some cases its projection on configuration space may be spatially very limited. Thus confined chaotic orbits may well contribute to the formation of galactic structures, even to ones which are narrow features in configuration space. Examples of such a case are the chaotic orbits guided by the manifolds in the outer parts of a strong bar. Although chaotic, these orbits are confined by the inner manifold branches and can thus outline the shape of the bar and its outer isodensities (see also Patsis *et al.* 1997; Voglis, Harsoula & Contopoulos 2007)

It is thus necessary to keep a broad view of what constitutes a building block of a galaxy. Indeed, we need to consider in all cases not only the regular orbits trapped around the stable periodic orbits, but also confined chaotic orbits. The latter have received

little attention so far and could bring new light to many galactic dynamics problems.

Let us now discuss separately the orbits in rings and in spirals. In the case of rings, a particle caught by a manifold stays there indefinitely<sup>3</sup>. This may seem in contradiction with the fact that the orbit is chaotic, but in fact it is not. Chaotic orbits indeed occupy all available phase space, but the projection of this space on to configuration space can be severely confined by regions with regular orbits. For example, if we take a chaotic orbit following the path outlined in panel c of Fig. 3, the configuration space available to it is confined from the inner part by the stable periodic orbits around  $L_4$ , by the regular orbits trapped around them and by the curve of zero velocity of the same energy as the orbit. Similarly, from outside the confinement comes from the stable periodic orbits at larger radii from the centre and from the regular orbits trapped around them. So the chaotic orbits trapped by the manifolds do occupy all the available phase space, but in this case the projection of the available phase space onto configuration space is of very limited extent. The important point to underline is that, in this case, the form of the available configuration space is just appropriate to reproduce the observed shapes of  $r$ ,  $R_1$ ,  $R_2$ , or  $R_1 R_2$  rings.

The case of spirals can be somewhat different. Let us again consider the case we have worked with so far, namely a rigid rotating bar potential. Again a particle which is trapped in a manifold will stay there indefinitely (in theory at least). But now the manifolds ‘widen up’ as they move away from the region around the Lagrangian point from which they emanate. This means that after one or more revolutions around the galactic centre (in the rotating frame of reference) the manifolds may be too wide to outline spiral arms. This can in practise limit the radial extent of the arm, but this limit is not sharp – contrary to the inner and outer Lindblad resonances which are sharp limits for non-driven stellar density waves (e.g. Lin 1967, for a review). The orbits will then, while still being in the manifold, contribute to the axisymmetric background rather than to the spiral arm. This has several implications.

The first one concerns response simulations in purely stellar cases with a rigid potential. Schwarz (1981) performed such simulations in which the bar was initially grown gradually and then kept at a constant amplitude and he found that the response was a spiral during the time when the bar was growing, but no spiral could be seen after that. This is indeed what our theory predicts and there is thus good agreement between our theory and these simulations. A second implication is that a particle has a ‘useful life’, during which it will contribute to the arm and after which it will contribute to the disc density. How this affects the life-time of spirals and whether these are long- or short-lived is discussed in Sect. 6.3.

## 6.3 Time evolution. Are spirals and rings long-lived, or short-lived?

In a galaxy we do not observe the manifolds themselves, but the material that is confined by them. Indeed, the manifolds are only the building blocks and thus may exist, but trap few or no orbits, in which case the corresponding structure will be very faint or even not visible in the galaxy. This is similar to the periodic orbits, which are the building blocks of bars and which need to trap regular orbits around them for the bar to form. In other words, the existence of a

<sup>3</sup> This is true in theory and for rigid potentials. For real galaxies, see Sect. 6.3

manifold is a necessary, but not a sufficient condition for the corresponding galactic structure to form. Thus, manifold theory without any information on the formation of the galaxy can answer questions concerning the shape of a spiral or a ring, but can give little or no information on its amplitude.

In a purely stationary model, material can not move in or out of a manifold. In a galaxy, however, a gas cloud or a star can do so after a collision (e.g. if it encounters another gas cloud), or if the bar potential or pattern speed change. Most of the material is expected to be trapped in a manifold as the bar forms and grows. Thus, in principle at least, information on how much material is contained in the manifold could be obtained by calculations including time evolution, so that the trapping of the material in the manifolds can be followed (Paper IV).

Are spirals in our theory short-lived or long-lived? Spirals will exist as long as there is sufficient material guided by the manifolds. As already discussed, this material comes from the bar region, is fed to the vicinity of the Lagrangian points by the inner stable branches of the manifolds and from there moves outwards along the arms to get dispersed in the outer parts of the galactic disc, due to the broadening of the manifolds. Thus the spiral will survive only as long as the reservoir (i.e. the outer parts of the bar and the vicinity of the Lagrangian points) is capable of providing fresh material. When this dries up, the spirals will fade out although the manifolds still exist. In this sense, the spirals can be considered as relatively short lived.

However, it is now well established from  $N$ -body simulations that bars evolve with time, getting longer and stronger while slowing down (Debattista & Sellwood 2000; Athanassoula & Misiriotis 2002; Athanassoula 2003, 2005; Valenzuela & Klypin 2003; O'Neill & Dubinski 2003; Debattista et al. 2006; Martinez-Valpuesta et al. 2006; Berentzen et al. 2007, etc.). The Lagrangian points move outwards and at the same time the outer parts of the bar occupy a different region of the galactic disc. Thus the mass reservoirs get replenished and they can feed mass to the spiral for longer times, although the form of these spirals will evolve with time (since the bar strength and  $r_L$  change). Further work (Romero-Gómez et al, in preparation) is necessary in order to estimate the bar evolution that can maintain a long-lived spiral, and whether any fine-tuning is necessary for this. So at this stage we can only present this as a possibility, but lack solid proof. To summarise, our theory predicts short lived spirals if the bar does not evolve, or evolves little, but could in principle predict relatively long lived but evolving spirals if the bar grows sufficiently with time. In no case do we get a long-lived stationary spiral. If for some reason the bar growth stops, the spiral will not survive for long and will not be visible after the reservoir has dried out. The rate at which new material needs to be provided depends on the instability of the Lagrangian points, i.e. on the strength of the bar.

The situation is different for rings. Fig. 3 shows the motion in an  $rR_1$  morphology. In such cases, once material is trapped by the manifolds, it can stay there indefinitely, if the potential does not change with time and if other forces (such as collisions, or dynamical friction) do not force it to leave the arm. Furthermore, if the potential evolves very slowly, the rings could follow it by adiabatically changing their shape. Thus, rings should be more long-lived than spiral arms and do not rely on strong secular evolution for their existence, but may adapt their properties to the bar evolution.

#### 6.4 Comparison with other spiral structure theories and with observations

According to our theory the building blocks of spirals and of rings in barred galaxies are chaotic orbits guided by the manifolds associated to the  $L_1$  and  $L_2$  Lagrangian points. This, however, is not the only alternative, and most spiral structure theories are based on the density wave concept initially introduced by Lindblad (1963). Grand design spirals can thus be driven e.g. by companions, or by bars, or perhaps be modes relying on some amplification mechanism. Flocculent spirals can be due to local swing amplification, while self-propagating star formation has also been proposed. Several origins for spirals are thus possible depending on the case (existence and relative orbit of the companion, existence of a strong bar, etc), so that spirals in different galaxies may have different origins. Furthermore, even in a single galaxy more than one mechanism can be at play. The properties of the resulting spiral would then result from the self-consistent interaction of all the spirals of different origins. Thus for example, the density from orbits trapped by the manifolds can help drive a response which will include orbits of energies other than the ones concerned by the manifolds discussed here, so that the resulting spiral will be somewhat different from what would be expected from the manifold theory alone.

Similarly, different alternatives can occur when we consider the fate of a gas cloud falling on a manifold arm. If the potential is evolving, i.e. the bar is growing, or if the motion of the cloud is perturbed by a collision with another cloud, it can be trapped by the manifold and continue its motion along the arm. Whether this will trigger star formation or not can not be answered here. On the other hand, if the cloud is not trapped by the manifold, it will cross the arm and its fate will be as described by Roberts (1969), i.e. there can be star formation and an age gradient roughly perpendicular to the arm.

Our theory leads naturally to a preference of two-armed grand-design trailing spirals in barred galaxies (Paper IV), in good agreement with observations. Other theories and other circumstances, however, may result in different spiral properties (see Toomre 1977; Athanassoula 1984, for reviews) and not all theories can show a preference for trailing two-armed spirals. Resonances aside, the WKBJ density wave dispersion relation does not discriminate between leading and trailing spirals, both being equally possible, while the WASER feedback cycle involves three waves, long or short but always trailing. Driven density waves have a given sense of winding depending on the driving agent. Namely, a growing bar will drive a trailing two-armed spiral, a directly rotating companion will drive mainly two-armed trailing spirals and a retrograde satellite a one-armed leading spiral. The swing amplifier feedback cycle relies on three waves, the two within corotation being one leading and the other trailing (Toomre 1981). The ratio of their amplitudes depends on the amplification factor. Within corotation, the superposition of the two waves will give an interference pattern (see e.g. figure 12 in Toomre (1981), or figure 31 in Athanassoula (1984)) and Fourier analysis should reveal the existence of the two components, provided of course the amplification factor is not too large. A similar statement can be made for our theory. If the ratio of the amount of material trapped in the unstable to the material trapped in the stable manifold is not too large, interference patterns will be clearly visible and the leading component will be detectable by Fourier analysis. In fact, this has been observed in a number of nearby galaxies (Athanassoula 1992c; Puerari et al 2000). On the other hand if the ratio is very large, then only the trailing component can be detected. Unfortunately these properties alone will not allow

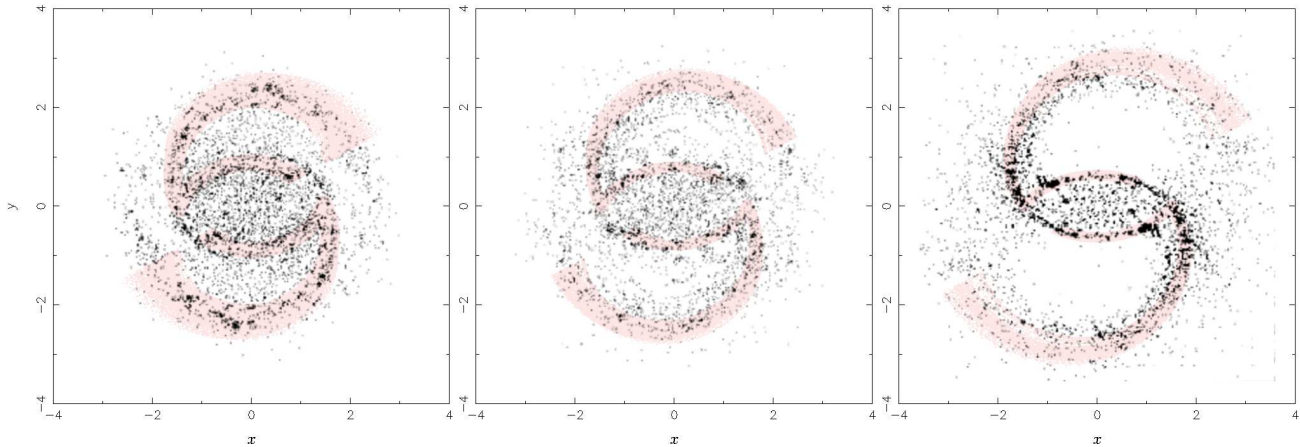


**Figure 12.** Comparison of the loci of gaseous manifolds to the gas response. The manifold loci are given in pink and the positions of the gas clouds in the response simulations in black. The latter are taken from Schwarz (1984). We make a comparison for three models with bars of different strengths, the bar strength increasing from the left to the right in the figure.

us to distinguish between the swing amplifier and the manifold origin of a spiral, since both theories can account for the presence or absence of a leading component and of interference patterns.

The bar strength affects the properties of the spirals in a different way in driven density waves and in our theory. In the former, and unless yet unknown nonlinear effects can modify this, the strength of the bar affects the amplitude of the spiral in the sense that stronger bars will drive higher amplitude spirals. In fact in a linear theory, the spiral amplitude is proportional to the bar strength. On the other hand in our theory the bar strength affects the pitch angle of the spiral, but not necessarily its amplitude, since the strength of the bar will change the manifold shape but may not affect its amplitude which depends only on how much mass the manifold traps. As discussed in Paper IV, it is not straightforward to test this fully with observations. Existing results, however, give us some crucial information. Thus, Seigar & James (1998) and Seigar, Chorney & James (2003) find that there is no correlation between bar and spiral strength. The question was revisited by Buta et al. (2009), using a sample of 177 galaxies and a different method for measuring the bar and the spiral strength. They find a very weak trend, with a linear correlation coefficient of 0.35 and a Kendall tau rank coefficient of 0.22. These numbers are so low that the existence of a trend is questionable. The lack of any trend or correlation was confirmed by Durbala et al. (2009), using Sb - Sc galaxies from the AMIGA sample of isolated galaxies (Verdes-Montenegro et al. 2005). Salo et al. (2009), however, argues again in favour of a correlation. The observational situation is thus still unclear. The existence of a correlation would be in good agreement with the linear density wave theory, while the lack of such a correlation would argue against it, at least in its current linear form. On the other hand, the theory we propose here, can not give definite information as to whether such a correlation should exist or not, unless further work concerning the trapping is made. Thus, the existence or the absence of such a correlation can neither confirm nor reject it.

Compared to density wave theory, our theory has a number of further advantages. It can explain the formation not only of spirals, but also of rings, and reproduce their main morphological properties. The continuity between rings and spirals follows naturally from our work, while it can not be explained by density wave theory. Our theory can also reproduce the shape of spiral arms such

as those of NGC 1365, NGC 1300, or NGC 1566 (see figures in e.g. Vera-Villamizar et al 2001), which ‘fall-back’ towards the bar region or towards the opposite arm (Sect. 2 of Paper IV), while this can not be reproduced by density wave theory.

This difference between the arm shapes as predicted by our theory and by density wave theory has a corollary. Namely, density wave theory predicts that velocities will be outwards in all the spiral arm region of a barred galaxy, since this region is beyond corotation. On the other hand, for our theory, these velocities will be outwards for most of the spiral extent, but will turn to inwards in the outermost part of the spiral, where the arm starts falling back towards the bar, or towards the other arm (see Sect. 4). These parts, however, are very low density, particularly for strong bars, so kinematical observations will not be easy to make. Furthermore, it is unclear at this stage how much this result will be affected by a self consistent estimate of the potential, although this may not be so important for such low density parts.

A further difference between the density wave theory and our theory, at least in its present non-selfconsistent version, could be found in the effect of the velocity dispersion. According to density wave theory, this will influence strongly the pitch angle of the arms, as has been shown in the local theory, in global modes and in response spirals (Kalnajs 1970; Lin & Shu 1971; Athanassoula 1978, 1980; Bertin et al. 1989; Hozumi 2003). As a stellar population becomes older, it will emit stronger in the IR and the NIR and less strongly in e.g. the blue wavelengths. At the same time its velocity dispersion will increase (e.g. Binney & Tremaine 2008), so that, all other parameters and properties remaining constant, its spirals should become considerably more open. Thus, according to the density wave theory, there should be a considerable difference between the winding of spirals as observed in the blue and in the NIR (for quantitative estimates see the above mentioned references). On the contrary, in our theory stars of different ages will trace the same spiral arm, i.e. they will be guided by the same manifold, if they have the same energy. Thus the only way for spirals viewed in different wavelengths to have a considerably different winding, is for the distribution of the energies of the stars, and particularly the mean energy, to depend strongly on age. Although a quantitative estimate of this dependence is not available at present, we wish to underline this as a useful subject for future work, since

it could shed some light on the differences between spirals due to a density wave and spirals due to our theory.

It should also be kept in mind that the corresponding observational test is not easy, since it is difficult to disentangle the effect of the velocity dispersion from that of other parameters. Yet the images of the S4G sample (Sheth et al. 2010) show that there is little, if any, difference between the winding of the arms in the blue and at  $3.6\mu\text{m}$  (Buta et al. 2010, and private communication), certainly much less than predicted by e.g. the estimates in Hozumi (2003). Furthermore, Buta et al. (2010) found that galaxies at  $3.6\mu\text{m}$  tend on average to appear “earlier” in type than in the blue, by approximately one stage. This argues against a statistical ‘opening’ of the arms as one goes from blue to mid-IR. Although further work is necessary in order to substantiate the above statements, these results show that there might be a potential problem with density waves in this respect, which the manifold theory would not suffer from.

In our theory, the bar and the spiral have the same pattern speed, contrary to some other theories, where more than one pattern speed can be present in the same disc galaxy (Tagger *et al.* 1987; Sellwood & Sparke 1988; Sygnet *et al.* 1988; Masset & Tagger 1997), so that the spiral can rotate with a different pattern speed from that of the bar. Unfortunately it is very difficult, if at all possible, to distinguish between these cases observationally. One possibility would be to check the position of the dust lane along the arm with respect to the arm centre, i.e. to check whether it is on the trailing or the leading side of the arm. Similarly one could check where the radial motion switches from inwards to outwards. Both, however, are very difficult to pinpoint. The task is further complicated by the fact that if the spiral potential is a sizeable part of the total, then the Lagrangian points are not on the bar major axis, but they move to a position somewhat further out along the arm. Thus, e.g. in NGC1365, the crossing of the dust lane from one side of the arm to the other does not necessarily imply that the spiral has a different pattern speed from that of the bar. Indeed, as discussed in Sect. 5, our theory, in which the bar and the spiral have the same pattern speed, can also explain this shift.

Work along lines similar to ours has also been carried out by others. Danby (1965) argued that bar orbits departing from the vicinity of the unstable Lagrangian points play an important role in the formation of the spiral arms. Kaufmann & Contopoulos (1996) linked chaotic orbits to the presence of spiral arms. This was further developed by Patsis (2006) with the help of response calculations in the potential of NGC 4314 (as calculated by Quillen, Frögel & Gonzalez (1994)) and by Voglis, Stavropoulos & Kalapotharakos (2006a) who used a potential from an  $N$ -body simulation. Manifolds were specifically referred to, although in a quite different way from that used in our work, by the late Prof. Voglis and his collaborators (Voglis, Tsoutsis & Efthymiopoulos 2006b). These authors consider only spirals –and not rings – and, as underlined by Tsoutsis et al (2009), they do not consider the swarm of orbits trapped by the manifolds, but the loci of their manifold apocentre. Due to the differences between our work and that of Voglis and his collaborators, our theoretical results and our comparisons with observations can not be straightforwardly extended to the Voglis et al. studies.

### 6.5 Comparison with response simulations

We can also compare our results with those of simulations. Since our calculations are not self-consistent, we will make comparisons

only with response simulations. Such comparisons can be even quantitative for simulations such as those of Schwarz (1979, 1981, 1984), where the gas clouds are modelled as colliding particles. We employed a similar technique when calculating the orbits in our manifolds (see Paper III for a technical description of the method) and we make a comparison with Schwarz’s results in Fig. 12. The three panels correspond to three models of different bar strength given in the lower panels of figure 1 of Schwarz (1984). The positions of the gas clouds in the simulation are given in black and the manifold loci in pink.

We see that the agreement is very good, particularly if we take into account that our treatment of collisions is very similar, but not identical to that of Schwarz, because we do not have a population of colliding clouds. Also, and for the same reason, the number of collisions we use is somewhat arbitrarily chosen. In the examples in Fig. 12 we took one collision per half bar rotation, but roughly equally good results can be found if the collision rate is doubled.

This argues that the orbits in Schwarz’s simulations are guided by manifolds such as those we discussed in our series of papers. This argument is further strengthened by further good agreement found between our results and those of Schwarz. For example, Schwarz (1981, 1984) finds that in his simulations  $R_1$  rings do not form in cases with strong bar forcings. Similarly, in his simulations he finds that stronger bars drive more open spirals than weaker bars. Both these simulation results have now been understood and explained with the help of our work (Paper III) and are a natural consequence of our theory.

In Papers II and III we showed that in the  $R_1R_2$  morphologies, material from the outer part of the bar fills in first the parts of the manifolds that correspond to the  $R_1$  morphology and only afterwards the  $R_2$  part. In other words, the  $R_1$  part of the morphology forms first and is followed by the  $R_2$ . This was indeed first seen in the response simulations of Byrd et al. (1994), who ran a large number of simulations very similar to those of Schwarz aiming to understand the evolution and morphology of the gaseous distributions in barred galaxies. This fact is also in good agreement with observations. Indeed, the Catalogue of Southern Ringed Galaxies (Buta 1995) has revealed the existence  $R_1R_2$  morphologies with  $R_1$  rings which are weak in blue light and very strong in the  $I$  band. A good example is IC1438.

More comparisons are of course necessary in order to fully establish the fact that the motions of particles in response simulations are guided by manifolds as the ones described in this series of papers. Nevertheless, the morphological agreement in Fig. 12 and in other models (not described here), as well as the other agreements presented in this series of papers, make this very plausible. If the correspondence between manifolds and simulation results is indeed established, the good agreement between response simulations and observations found for many galaxies (e.g. Buta, Crocker & Byrd 1999; Salo *et al.* 1999; Rautiainen, Salo & Laurikainen 2005; Treuhardt, Salo & Buta 2009) will also be found when comparing the observations to the manifold loci in the appropriate potentials.

### 6.6 Future work

In this series of papers we developed some basic aspects of our theory and compared it to observations. We used simple rigid potentials in which we calculated manifolds and orbits. This allowed us to get a good understanding of the underlying dynamics and its applications and showed that the theory we propose can play a crucial role in explaining the formation and properties of spirals and rings in barred galaxies. We will outline here a number of avenues

for future research which should contribute further to assessing our theory and to extending it to other types of spirals and other configurations.

We have so far developed the theory only for the case of saddle point Lagrangian points. Yet the contribution of confined chaos to the morphology and structure of galaxies extends much further than this. For example, in Sect. 4.2 of Paper IV we saw that the  $L_4$  and  $L_5$  Lagrangian points can become complex unstable for very strong Ferrers bars. It is thus necessary to understand whether and in which way the corresponding manifolds can, in such cases, contribute to galactic morphology. Also, most families of periodic orbits include at least some energy ranges with unstable orbits, whose orbits can not trap material. In such cases as well, confined chaos and manifolds may contribute to create morphological features. Considerable theoretical work is still necessary to fully explore all these theoretical aspects.

So far we have used three types of bar potentials, the Ferrers (in model A, Ferrers 1877), the Dehnen (in model D, Dehnen 2000) and the Barbanis-Woltjer (in model BW, Barbanis & Woltjer 1967) potentials. The two last ones are ad hoc, but have the big advantage of providing a considerable non-axisymmetric force beyond corotation. Ferrers bars correspond to a realistic projected density distribution, but their non-axisymmetric force beyond corotation decreases strongly with radius and their vertical mass distribution is oversimplified. It would thus be both straightforward and useful to extend this work to other potentials.

We need to check how different potentials affect the various correlations and trends we found and whether these become substantially broader when results from many different but all realistic potentials are used. But the number of possible potentials is very large and we can never be sure that we have covered all the relevant ones, while some of the potentials may be unrealistic and thus introduce an artificial broadening. Thus a better possibility, outlined already in Paper II, is to calculate potentials directly from galaxy images and the galaxy rotation curve, the former preferably in a wavelength tracing the old stellar population (e.g. Lindblad, Lindblad & Athanassoula 1996; Salo *et al.* 1999; Kranz, Slyz & Rix 2003; Perez, Fux & Freeman 2004; Byrd, Freeman & Buta 2006; Rautiainen, Salo & Laurikainen 2008). Although this is in principle straightforward, it still has two considerable drawbacks. The first one is that even in the near infrared a non-negligible fraction of the light is contributed by young stars and not from the old underlying stellar population and is not easy to eliminate. The second difficulty comes from the fact that we observe galaxies as projected on the sky and have no information on their three-dimensional structure, other than by extrapolating from similar galaxies seen at other orientations. Two identical projected density distributions can, however, have considerably different three dimensional density distributions and potentials. This introduces a particularly serious drawback in the bar region. Indeed we know that, seen edge-on, bars are vertically thin only for a short time after their formation and afterwards most of their extent acquires a boxy or peanut shape which extends vertically well above and below the galactic disc (see e.g. Athanassoula 2008, for a review). This can introduce non-negligible errors in the calculation of bar potentials and forcings from near infrared images. Even so, potentials stemming directly from observations can be most useful for calculating orbits and manifolds, since it is guaranteed that, to a first approximation, they correspond to realistic density distributions.

There is a further way in which potentials should be improved, namely by including evolution. Indeed it is well known that barred

galaxies evolve and thus it would be useful to calculate manifolds in evolving, i.e. time dependent potentials. Such work is underway (Romero-Gómez *et al.* in preparation).

Even a perfect potential, however, can give only qualitative information about the orbits that constitute it and can not reveal whether a given manifold guides a sufficient number of orbits for a structure to be observable. Such information on the orbits can come only from  $N$ -body simulations, or from methods such as the Schwarzschild method and its extensions (Schwarzschild 1979; Syer & Tremaine 1996; de Lorenzi *et al.* 2008; Dehnen 2009, *etc.*), or the iterative scheme (Rodionov, Athanassoula & Sotnikova 2009). Such methods provide initial conditions for orbits, thus making it possible to test whether the latter are trapped by the manifolds.

Finally, a most important contribution to assessing our theory will come from further comparisons with observations and by checking out the observational predictions made in this series of papers.

## 7 SUMMARY AND CONCLUSIONS

Since the early work of B. Lindblad (1963), density waves have been commonly assumed to be at the basis of any explanation of spiral structure formation. In this series of papers we presented an alternative viewpoint, which we have applied specifically to barred galaxies. This explains the formation of spiral arms, as well as of inner and outer rings, in a common theoretical framework. According to our theory, it is the unstable Lagrangian points located at the ends of the bar and the corresponding manifolds that are responsible for the formation of spirals and rings. These manifolds drive orbits, which are in fact chaotic, but are confined by the manifolds, so that they create over-densities which have the right shape to explain the spirals and the rings (Papers I and II).

We showed that weaker non-axisymmetric perturbations will produce manifolds of  $R_1$  ring shape, while stronger ones will produce other types of rings and spirals. It is, nevertheless, the same theory that can explain all these different morphologies. This is in good agreement with the observed morphological continuity between rings, pseudorings and spirals. This continuity is clear in our theory, but not in others.

We made many different kinds of comparisons with observations. We first made sure that our theory can account for the basic morphological structures observed, namely the spirals, the inner rings and the outer rings (Paper IV). The model outer rings have the observed  $R_1$ ,  $R_2$  and  $R_1 R_2$  ring and pseudo-ring size and morphologies, including the dimples often observed near or at the direction of the bar major axis. Both model and observed inner rings have roughly the same relative sizes and orientations.

We next turned to the main spiral arm properties (Paper IV). We showed that, as the bar grows, material gets trapped mainly in the unstable manifolds, i.e. the sense of the arms will be trailing, in good agreement with what is currently known from observations. There is, nevertheless, a very small fraction of the material concerned that will be caught by the stable manifold branch, and will thus form a very low amplitude leading spiral. If its amplitude is not too low, it may be observable in a Fourier analysis of the galaxy image, or as interference patterns on the arm amplitude.

Theoretical and observational results agree also well on the number of arms in a barred galaxy (Paper IV). Our theory links one spiral arm to each of the unstable Lagrangian points in the standard case. Since galactic bars are bisymmetric, there should be two such

Lagrangian points, the  $L_1$  and  $L_2$ , and therefore two spiral arms. This morphology persists even in the non-standard case where the  $L_1$  and  $L_2$  are stable (Paper III). Indeed, the vast majority of barred galaxies have two spiral arms. There are, nevertheless, a few barred galaxies with four spiral arms. Our theory can account for such cases, given the right potential, and we discussed a few such potentials in Paper IV.

We also compared the shape of observed spiral arms with those of manifolds (Paper IV). We showed that our theory can explain the characteristic arm winding often observed, namely that, as the angle along the arm increases, the radius first increases and then, after reaching a maximum, ‘falls back’ towards the bar. This property has, to our knowledge, not been reproduced by any other theory so far, but follows naturally from ours. We also predict that spirals in galaxies with stronger bars will be more open than those in galaxies with weaker bars. This prediction can be made because our theory, contrary to most others, is non-linear. Finally, very tightly wound near-logarithmic spirals can also be obtained with our theory, but will rely considerably on spiral forcing.

The shape of rings and the ratio of their extents, although not as straightforward to compare as other properties, reveal interesting information (Paper IV). Concerning  $R_1$  rings, for which we have sufficient models to get adequate statistics, we find that the ring shapes cover the same range as observations. A comparison for inner rings is less straightforward, because in strong bar cases parts of the inner manifold branches outline parts of the bar and not an inner ring. Taking this into account, we find that there is a fair agreement between models and observations.

One of the predictions made in Paper IV concerns the shape of the inner rings. Namely, we found a strong correlation between the ring shape and  $Q_{t,L_1}$ , in the sense that bars with a stronger forcing at or somewhat beyond  $L_1$  should have more elongated  $R_1$  rings. We also stressed that, in order for correlations concerning a spiral or a ring property with the strength of the non-axisymmetric forcing to be strong, the latter quantity should be measured at or beyond the Lagrangian radius, i.e. with  $Q_{tL_1}$ . If  $Q_b$  is used instead, the correlation can be destroyed, or severely damaged. Both of these results have now been confirmed by observations (Grouchy et al. 2010).

We also introduced collisions and dissipation to the manifold calculations, in order to roughly model the gas properties (Paper IV). We found that this does not influence the existence of the spiral arms or rings, and makes no major modifications to their shape. The amount of dissipation, however, does influence the width of the arms. These become thinner as the dissipation is increased, so that the gaseous arm comes nearer to the lowest energy manifold.

Our theory makes very clear and, for many morphological types, precise predictions about the value of the bar pattern speed, since it shows how it is possible from the morphology only to locate the positions of the  $L_1$  and  $L_2$ , both for spirals and for the various ring morphologies (Paper V). This of course works only in the case where sufficient morphological features are present in the observed galaxy. For example if there is only a bar, with no spirals or rings, our theory can not be applied and the  $L_1$  and  $L_2$  can not be located. However, in cases with a reasonable amount of structure our theory allows the location of the  $L_1$  and  $L_2$  from morphology alone. In cases with appropriate morphological features this may allow a more accurate determination of the pattern speed than other methods used so far. Our theory also provides building blocks to explain the rectangular-like outline observed in strong barred galaxies and to explain ansae (Paper V).

Concerning photometry, our results are not very constraining.

The amplitude of the spiral should in general decrease outwards, but this decrease may well not be monotonic, because other arm components – e.g. a weak, leading component –, if present, will lead to bumps on an otherwise smoothly decreasing density profile.

The circulation of material within the manifolds also depends on the bar strength. In the relatively weak bars, which form  $rR_1$  morphologies, the mass elements can move from the inner manifolds to the outer manifolds and then back to inner ones again. I.e. material can move from the region within corotation to the region outside it and vice versa via the neighbourhood of the  $L_1$  and  $L_2$ . Averaged over time, this brings internal circulation, but no net motion of material inwards or outwards. The situation is more complex for the cases where the non-axisymmetric forcing around corotation is stronger and which have a spiral morphology. In such cases, material moves from the region within corotation to the region outside it. If the potential has a predominantly barred structure, this material returns eventually to the region of the bar or of the other arm. But if the potential has also a spiral component, then the arm can continue winding outwards for much longer times. Either way, this results in a considerable radial mixing and material can reach the outermost parts of the disc and can contribute to its radial extension. Of course the density wave theory had already predicted that in a spiral galaxy the radial motion is outwards outside corotation (Lin & Shu 1971; Kalnajs 1978). Our results, however, are more than a simple restatement of the above, because our theory shows how material from well within corotation can reach regions well outside it. It can thus explain considerable radial mixing and have a more important impact on the formation of the outer disc than those of the density wave theory. Furthermore, our theory predicts the relation between bar strength and the abundance gradients found in observations (Martin & Roy 1994).

We also made predictions on the galaxy kinematics, by measuring the radial and tangential velocity components along the manifold loci, i.e. along the spirals and the inner and outer rings. For the tangential component we subtract the local circular velocity and thus obtain the perturbation, or peculiar tangential velocity. Plotted as a function of the azimuthal angle along the ring, both radial and tangential velocities show  $m = 2$  oscillations, the amplitude of the former being higher than that of the latter. We find that the amplitude of these oscillations increases with increasing bar strength and that they are larger in the inner than in the outer ring. The latter result is in agreement with the former, since the bar forcing is higher at the inner ring than at the outer one.

For spirals, we find that the radial velocity of material moving from the Lagrangian points outwards along the arm increases with the distance to the Lagrangian point until it reaches a maximum and then it decreases, until at some point it changes sign. From that point onwards the arm will start approaching the other arm or the region of the bar. Where this occurs is a function of the bar strength and, when observed, will provide an additional confirmation to our theory. Nevertheless, this may be a difficult observation to make, since the spiral density is low in that region. Furthermore, in galaxies with a high spiral amplitude, the spiral forcing may be a considerable fraction of the non-axisymmetric forcing, so that this sign reversal may not take place. Finally, we calculated the line-of-sight velocity and found that in the case of rings its variation along the ring can be well modelled by a sinusoidal. This is not true for very strong bars and spiral morphologies. Finally, when the sinusoidal is a reasonable fit, we find that the difference between the kinematic and photometric major axes is in agreement with the observed values.

As already mentioned, our models show a clear connection

between bar strength and morphology of the response. Relatively weak non-axisymmetric forcings give  $R_1$  and  $R'_1$  morphologies, while stronger forcings give spirals and other types of rings. Yet it is possible in self-consistent calculations, in which the potential due to the material trapped in the manifold is taken into account, to form a spiral in cases where the bar on its own is too weak to sustain it. This is due to the fact that initially the only part of the ring that will be populated is the part which is near the  $L_1$  or the  $L_2$ . This then adds a spiral-like forcing to that of the bar, so that manifold will have a more spiral-like shape. It is thus possible in self-consistent calculations to have a spiral morphology in a bar potential which is somewhat below the threshold between the  $R_1$  and the spiral morphology in the rigid bar forcing case.

In these series of papers, we applied our theory to barred galaxies. It can, however, be straightforwardly applied also to non-barred galaxies with other non-axisymmetric perturbations, such as spirals or ovals, provided these have unstable saddle Lagrangian points. There is thus no discontinuity between barred and non-barred spiral galaxies. On the other hand it is unclear at this point whether, and under what conditions, complex unstable Lagrangian points can have the type of manifolds that can create realistic spirals or rings. Such Lagrangian points are found e.g. at the  $L_4$  and  $L_5$  Lagrangian points of very strong bars (Athanasoula 1992a, and Paper IV). More work is necessary before this question can be answered.

We discussed how material can get trapped in the manifolds, where the mass in the spirals comes from and whether the spirals are short-lived or long-lived. We also compared our theory with other theories not relying on chaotic orbits and manifolds. In particular, we discussed a number of advantages which our theory has over the density wave theory. We stressed that it need not necessarily be the same theory that explains all spirals in disc galaxies, and even in one single galaxy more than one mechanism can be at play. The properties of the resulting spiral would then result from the self-consistent interaction of all the spirals of different origin. We finally propose a number of avenues for future work within the framework of our theory.

We showed that the orbits that form the building blocks of the spirals and of the inner and outer rings are chaotic. Nevertheless, they can form narrow features because they are confined by the manifolds, which act as guiding tubes. We propose to call this type of chaos ‘confined chaos’ and suggest that such orbits should be taken into account in dynamical studies, since they could contribute, together with the regular orbits trapped around the stable periodic orbits, to galactic structures.

A prerequisite for any theory is that it can be falsified (e.g. Popper 1959). Ours fulfils well this criterion. Indeed there are a number of observational results that could have proved it wrong. Namely, if the two armed global spirals were not preponderant in symmetric barred galaxies, or if these arms were leading, or if the major features of the observed and the theoretical morphologies were inconsistent, our theory would have been proven wrong. As we showed in this paper, this is not the case and there is good agreement between our theory and observations in these and many other points. There are more observations which could have proven our theory to be wrong. For example, our theory would be invalidated if it was clearly shown that all spirals rotate with a different pattern speed than the bar.

In total over the five papers, we presented a number of predictions of our theory. Whenever the necessary data are available, we compared the results of our theory to the existing observational results. All tests we have been able to make tend to show that our

theory is viable. In many cases, however, new observations, or new analysis of existing data are necessary. In such cases, we presented here simply the theoretical predictions and outlined the way the comparisons could be made. The results of these comparisons will be very important in order to confirm our theory, to bring about modifications, or to reject it. As already mentioned, one of the theoretical predictions of paper IV concerning the dependence of the inner ring shape on bar strength has already been confirmed by observations (Grouchy et al. 2010).

We can thus conclude that the theory we presented in this series of papers should be useful in order to explain the formation of spirals and of inner and outer rings in barred galaxies. Concerning rings, no other theory has been fully developed, while our results agree very well with those of simulations, suggesting that the motion of particles in them are guided by the manifolds we describe here. Concerning spirals, the comparisons we have made with observations are more extensive than those that have been made so far for the swing amplifier theory. Furthermore, our theory is clearly falsifiable, contrary to the classical WKBJ density wave theory (see discussion by Kalnajs (1978)). We thus believe that it should be considered as a possible alternative, on a par with other theories. More work, both theoretical and observational, is necessary in order to establish in what cases each one of the so far proposed theories prevails and how they can, perhaps all together, come to an explanation of spiral formation and spiral properties.

## ACKNOWLEDGEMENTS

EA thanks Scott Tremaine for a stimulating discussion on the manifold properties. We also thank Ron Buta, A. Mel’nik and P. Rautiainen for very useful discussions and email exchanges. This work was partly supported by grant ANR-06-BLAN-0172 and by the MICINN-FEDER grant MTM2009-06973, CUR-DIUE grant 2009SGR859 and MICINN grant AYA2009-14648-C002-01.

## REFERENCES

- Aguerre, J. A. L., Debattista, V. P., Corsini, E. M. 2003, MNRAS, 338, 465
- Athanasoula, E. 1978, A&A, 69, 395
- Athanasoula, E. 1980, A&A, 88, 184
- Athanasoula, E. 1984, Phys. Rep., 114, 319
- Athanasoula, E. 1991, in ‘Dynamics of disk galaxies’, B. Sundelius (ed.), Göteborg, Univ. Göteborg, 149
- Athanasoula, E. 1992a, MNRAS, 259, 328
- Athanasoula, E. 1992b, MNRAS, 259, 345
- Athanasoula, E. 1992c, in ‘Morphological and Physical Classification of Galaxies’, eds. G. Longo, M. Capaccioli & G. Busarello, Dordrecht:Kluwer, Astr. & Sp. Sc. Library, 178, 127
- Athanasoula, E. 1996, in ‘Spiral Galaxies in the NIR’, D. Minniti & H.-W. Rix (eds.), Berlin, Springer, 147
- Athanasoula, E. 2003, MNRAS, 341, 1179
- Athanasoula, E. 2005, Cel. Mech. & Dyn. Astr., 91, 9
- Athanasoula, E. 2008, in *Formation and Evolution of Galaxy Bulges*, eds. M. Bureau, E. Athanasoula and B. Barbuy, IAU Symposium 245, 93
- Athanasoula, E., Misiriotis, A. 2002, MNRAS, 330, 35
- Athanasoula, E., Morin, S., Wozniak, H., Puy, D., Pierce, M. J., Lombard, J., Bosma, A. 1990, MNRAS, 245, 130

- Athanassoula, E., Romero-Gómez, M., Bosma, A., Masdemont, J.J. 2009b, MNRAS, 400, 1706 (Paper IV)
- Athanassoula, E., Romero-Gómez, M., Masdemont, J.J. 2009a, MNRAS, 394, 67 (Paper III)
- Barbanis, B., Woltjer, L. 1967, ApJ, 150, 461
- Berentzen, I., Shlosman, I., Martinez-Valpuesta, I., Heller, C. 2007, ApJ, 666, 189
- Bertin, G., Lin, C. C., Lowe, S. A., Thurstans, R. P. 1989, ApJ, 338, 78
- Binney, J., Tremaine, S. 2008, Galactic Dynamics, Princeton Univ. Press, Princeton, 2nd edition
- Buta, R. 1986, ApJ, 61, 631
- Buta, R. 1987, ApJS, 64, 383
- Buta, R. 1995, ApJS, 96, 39
- Buta, R., Crocker, D. A., Byrd, G. G. 1999, AJ, 118, 2071
- Buta et al. 2009, AJ, 137, 4487
- Buta et al. 2010, ApJS, submitted
- Byrd, G., Freeman, T., Buta, R., 2006, AJ, 131, 1377
- Byrd, G., Rautiainen, P., Salo, H., Buta, R., Crocker, D. A. 1994, AJ, 108, 476
- Contopoulos, G. 1980, A&A, 81, 198
- Contopoulos, G. 1988, A&A, 201, 44
- Contopoulos, G. 2002, Order and Chaos in Dynamical Astronomy, Springer Verlag, Berlin
- Corsini, E. M., Debattista, V. P. 2010, 'Tumbling, twisting, and winding Galaxies: Pattern Speeds along the Hubble Sequence', Memorie della Societa Astronomica Italiana, in press
- Danby, J. M. A. 1965, AJ, 70, 501
- de Lorenzi, F., Debattista, V. P., Gerhard, O., Sambhus, N. 2007, MNRAS, 376, 71
- Debattista, V. P. et al. 2006, ApJ, 645, 209
- Debattista, V. P., Sellwood, J.A. 2000, ApJ, 543, 704
- Dehnen, W., 2000, AJ, 119, 800
- Dehnen, W. 2009, MNRAS, 395, 1079
- Durbala, A., Sulentic, J. W., Buta, R., Verdes-Montenegro, L. 2009, ApJ, in press and astro-ph 0905.2340
- Duval, M. F., Athanassoula, E. 1983, A&A, 121, 297
- Elmegreen, B.G. 1996, in 'Barred Galaxies', eds. R. Buta, D. A. Crocker & B. G. Elmegreen, PASP, 91, p. 197
- Ferrers N. M. 1877, Q.J. Pure Appl. Math., 14, 1
- Gadotti, D., 2008, in 'Chaos in Astronomy', G. Contopoulos and P. Patsis (eds), Springer Berlin Heidelberg, 159
- Gadotti, D., 2010, MNRAS, submitted and arXiv:1003:1719
- Gerssen, J., Kuijken, K., Merrifield, M. 2003, MNRAS, 345, 261
- Gómez, G., Koon, W.S., Lo, M. W., Marsden, J. E., Masdemont, J. J., Ross, S. D. 2004, Nonlinearity, 17, 1571
- Grouchy, R. D., Buta, R. J., Salo, H., Laurikainen, E. 2010, AJ, submitted and arXiv:1004.5063
- Hozumi, S. 2003, in 'Galaxies and Chaos', eds. G. Contopoulos and N. Voglis, Lecture Notes in physics 626, Springer Verlag, Berlin, 380
- Jörsäter, S., van Moorsel, G. A. 1995, AJ, 110, 2037
- Kalnajs, A. J. 1970, in 'The Spiral structure of our Galaxy', Symposium U.A.I. No 38, eds. W. Becker & G. Contopoulos, Reidel, Dordrecht, 318
- Kalnajs, A. J. 1978, in 'Structure and properties of nearby galaxies', Symposium U.A.I. No 77, eds. E. Berkhuisen & R. Wielebinski, Reidel, Dordrecht, 113
- Kaufmann, D.E., Contopoulos, G. 1996, A&A, 309, 381
- Koon, W. S., Lo, M. W., Marsden, J. E., Ross, S. D. 2000, Chaos, 10, 2, 427
- Kranz, T., Slyz, A., Rix, H.W. 2003, ApJ, 586, 143
- Lin, C. C. 1967, ARA&A, 5, 453
- Lin, C. C., Shu, F. H.-S. 1971, in 'Astrophysics and General Relativity', Brandeis University lecture series in theoretical physics, eds. M. Chretien, S. Deser and J. Goldstein, Gordon and Breach, New York, 235
- Lindblad, B. 1963, Stockholms Observatorium Ann., Vol. 22, No. 5
- Lindblad, P. A. B., Lindblad, P. O., Athanassoula, E. 1996, A&A, 313, 65
- Lyapunov, A. 1949, Ann. Math. Studies, 17
- Martin, P., Roy, J.-R. 1994, ApJ, 424, 599
- Martinez-Valpuesta, I., Knapen, J. H., Buta, R. 2007, AJ, 134, 1863
- Martinez-Valpuesta, I., Shlosman, I., Heller, C. 2006, ApJ, 637, 214
- Masset, F., Tagger, M. 1997, A&A, 322, 442
- Mel'nik, A., M., Rautiainen, P. 2009, Astronomy Letters, 35, 609
- O'Neill, J. K., Dubinski, J. 2003, MNRAS, 346, 251
- Ondrechen, M. P., van der Hulst, J. M. 1989, ApJ, 342, 29
- Patsis, P.A. 2006, MNRAS, 369, L56
- Patsis, P., Athanassoula, E., Quillen, A. C. 1997, ApJ, 483, 731
- Pérez, I., Fux, R., Freeman, K. 2004, A&A, 424, 799
- Popper, K. R. 1959, The Logic of Scientific Discovery. Hutchinson of London, London.
- Puerari, I., Block, D. L., Elmegreen, B. G., Frogel, J. A., Eskridge, P. B. 2000, A&A, 359, 932
- Quillen, A. C., Frögel, J., Gonzalez, R. 1994, ApJ, 437, 162
- Rautiainen, P.; Salo, H.; Laurikainen, E. 2005, ApJ, 631, 129
- Rautiainen, P.; Salo, H.; Laurikainen, E. 2008, MNRAS, 388, 1803
- Roberts, W. W. 1969, ApJ, 158, 123
- Rodionov, S. A., Athanassoula, E., Sotnikova, N. Ya. 2009, MNRAS, 392, 904
- Romero-Gómez, M., Masdemont, J.J., Athanassoula, E., García-Gómez, C. 2006, A&A, 453, 39 (Paper I)
- Romero-Gómez, M., Athanassoula, E., Masdemont, J.J., García-Gómez, C. 2007, A&A, 472, 63 (Paper II)
- Romero-Gómez, M., Masdemont, J.J., García-Gómez, C., Athanassoula, E. 2009, Communications in Nonlinear Science and Numerical Simulations, 14, 4123
- Salo, H., Laurikainen, E., Buta, R. J., Knapen, J. 2009, AAS abstract, meeting 214, 603.05
- Salo, H., Rautiainen, P., Buta, R., Purcell, G. B., Cobb, M.L., Crocker, D. A., Laurikainen, E. 1999, AJ, 117, 792
- Sandage, A. 1961, The Hubble Atlas of Galaxies (Washington: Carnegie Institution)
- Schwarz, M.P. 1979, Ph.D. Thesis, Australian National University
- Schwarz, M. P. 1981, ApJ, 247, 77
- Schwarz, M. P. 1984, MNRAS, 209, 93
- Schwarzschild M., 1979, ApJ, 232, 236
- Seigar, M. S., Chorney, N. E., James, P. A. 2003, MNRAS, 342, 1
- Seigar, M. S., James, P. A. 1998, MNRAS, 299, 685
- Sellwood, J. A., Sparke, L. S. 1988, MNRAS, 231, 25
- Sheth et al, 2010, PASP, submitted
- Skokos, Ch., Patsis, P. A., Athanassoula, E. 2002, MNRAS, 333, 847
- Syer, D., Tremaine, S. 1996, MNRAS, 282, 223
- Sygné J.F., Tagger M., Athanassoula E., Pellat R. 1988, MNRAS, 232, 733
- Tagger M., Sygné J. F., Athanassoula E., Pellat R. 1987, ApJ, 318, L43
- Toomre, A. 1977, ARAA, 15, 437



- Toomre, A., 1981, in 'The structure and evolution of normal galaxies', S. M. Fall & D. Lynden-Bell (eds), Proc. of the Advanced Study Institute, Cambridge, England, Cambridge University Press, Cambridge and New York, 111
- Tremaine, S., Weinberg, M. D. 1984, ApJ, 282, L5
- Treuthardt, P., Salo, H., Buta, R. 2009, AJ, 137, 19
- Tsoutsis, P., Kalapotharakos, C., Efthymiopoulos, C., Contopoulos, G. 2009, A&A, 495, 743
- Valenzuela, O., Klypin, A. 2003, MNRAS, 345, 406
- Vera-Villamizar, N., Dottori, H., Puerari, I., de Carvalho, R. 2001, ApJ, 547, 187
- Verdes-Montenegro et al. 2009, A&A, 436, 443
- Voglis, N., Stavropoulos, I., Kalapotharakos, C., 2006, MNRAS, 372, 901
- Voglis, N., Tsoutsis, P., Efthymiopoulos, C. 2006, MNRAS, 373, 280
- Voglis, N., Harsoula, M., Contopoulos, C. 2007, MNRAS, 381, 757
- Zanmar Sánchez, R., Sellwood, J. A., Weiner, B. J., Williams, T. B. 2008, ApJ, 674, 797